W. Scott Enochs, MD, PhD • Paul Petherick, BS • Anna Bogdanova, PhD • Ursula Mohr, MD
Ralph Weissleder, MD, PhD

Paramagnetic Metal Scavenging by Melanin: MR Imaging[1]

PURPOSE: To quantitate the binding of metals to synthetic melanin in vitro, which is believed to be the reason why melanotic melanomas are hyperintense on T1-weighted magnetic resonance (MR) images, and to test whether such binding by natural melanin can be detected in cultured melanoma cells in vivo with MR imaging.

MATERIALS AND METHODS: Seven synthetic metallomelanins were prepared and their metal contents and relaxivities determined. Melanotic PC1A and amelanotic B16 melanoma cells were incubated with increasing concentrations of iron. MR images of synthetic melanin and cell phantoms were obtained.

RESULTS: The iron-binding capacities and relaxivities of the different synthetic metallomelanins varied considerably, which reflects the heterogeneous structure of melanin and the complexity of its binding of metals. Nevertheless, the MR signal intensities of the synthetic melanin and cell phantoms show marked increases that scale, respectively, with increasing iron content and iron concentration in the incubation medium.

CONCLUSION: Melanotic melanomas are hyperintense on T1-weighted images because of paramagnetic metal scavenging. This observation has implications for the interpretation of MR images, the improved detection of melanomas, and the development of imaging marker genes.

MELANOTIC melanomas commonly have high signal intensities on T1-weighted magnetic resonance (MR) images (1–5); this is in contrast to most tumors, which have low signal intensities. This paramagnetic effect typically has been attributed to the free radicals known to occur in melanin (1,3–6). However, it has been shown by using synthetic models that the content of free radicals in melanin (10^{18} spins per gram or one free radical per 3,000 subunits) at the average concentration of melanin estimated within melanoma tissue (15 mg/mL) is too low to substantially affect the tissue T1 relaxation time (7).

Melanin also has a high affinity and binding capacity for metal ions (6 × 10^{20} sites per gram of melanin or one site for every five subunits) (8–10), and natural melanin contains a wide variety of bound metals in vivo (iron, copper, manganese, and zinc) (11–14), which indicates that melanin may have a cytoprotective function as an intracellular scavenger of free metals (15). We and others (7,16,17) hypothesize that it is the binding of paramagnetic metals that is responsible for the high signal intensities of melanomas on T1-weighted MR images. The present study was undertaken to (a) quantitate the paramagnetic metal-binding capacities of several melanins synthesized in vitro, (b) identify the detection threshold of such melanin-bound paramagnetic metals at MR imaging, and (c) test the hypothesis that metal binding to natural melanin indeed occurs in cultured melanotic melanoma cells.

MATERIALS AND METHODS

Chemicals

L-3,4-dihydroxyphenylalanine (L-dopa), mushroom tyrosinase, N-methyl-D-glucamine (meglumine), gelatin, agarose, and all other chemical reagents were obtained from Sigma Chemical (St Louis, Mo). Ferric chloride ($FeCl_3 \cdot 6H_2O$) was obtained from EM Sciences (Gibbstown, NJ), and cupric chloride ($CuCl_2 \cdot 2H_2O$) was obtained from Mallinckrodt (Paris, Ky). All cell culture reagents were obtained from Cellgro Mediatech (Washington, DC), and all cell culture plasticware from Falcon (division of Beckton Dickinson, Lincoln Park, NJ).

Melanin Synthesis

We have synthesized various melanin samples without (melanin samples 1 and 2) and with (melanin samples 3–9) metal ions (Table). Melanin samples 1–7 were prepared from L-dopa by means of autooxidation; melanin samples 8 and 9 were prepared by means of enzymatic oxidation with tyrosinase by using stochiometric ratios of substrates and reaction conditions that were chosen empirically but generally were based on prior protocols (18–20). The basic synthesis of melanin samples 1–7

Metallomelanin Preparations

Melanin Sample	Preparation	Metal Present during Synthesis	Metal Added after Synthesis	Molar Ratio of Metal to Monomer*	pH during Metal Exposure	Meglumine Stabilization	Metal Content (mg metal per mg solid)	R1 (mmol metal · L^{-1} · sec^{-1})	R2 (mmol metal · L^{-1} · sec^{-1})
1	Autooxidation	None	None	NA	8	No	NA	NA	NA
2	Autooxidation	None	None	NA	8	Yes	NA	NA	NA
3	Autooxidation	Fe	None	3.5	8	No	0.11 Fe	1.02	1.32
4	Autooxidation	Fe	None	1.9	8	Yes	0.16 Fe	0.34	0.43
5	Autooxidation	Cu	None	3.8	8	Yes	0.35 Cu	0.03	0.06
6	Autooxidation	None	Fe	0.6	2	Yes	0.08 Fe	0.37	0.51
7	Autooxidation	None	Fe	0.6	8	Yes	0.03 Fe	0.91	1.52
8	Enzymatic oxidation	None	Fe	0.6	2	Yes	0.13 Fe	0.08	0.27
9	Enzymatic oxidation	None	Fe	0.6	8	Yes	0.10 Fe	0.14	0.24

Note.—NA = not applicable.
* Monomer = concentration of dopa in initial reaction mixture for melanin samples 3–5 and the estimated concentration of subunits in preformed melanin for melanin samples 6–9, assuming an average subunit molecular weight of 154 (7).

consisted of dissolving 30–50 mg of dopa in 200 mL (8–13 mmol/L) of deionized, distilled water and continuously aerating the solution for 3 days while maintaining the pH at 8 by using concentrated NH$_4$OH. For melanin samples 8 and 9, 500 mg of L-dopa was dissolved in 100 mL of phosphate buffer (0.1 mol/L, pH 6.5; final concentration of L-dopa, 25 mmol/L), and 6 mg of mushroom tyrosinase was added. The solution also was aerated continuously for 3 days.

On the 4th day, all of the melanin solutions were exhaustively dialyzed (Spectrophor tubing; Thomas, Philadelphia, Pa; 12,000–14,000 MW cutoff) against one of the several dialysates described below; they were then lyophilized in a lyophilizer (Virtis, Gardiner, NY) for later use. Melanin 1 was prepared by means of alkaline autooxidation without modification to the basic protocol above and thus served as the primary control; the total yield was 1 g (17%).

The synthesis of melanin samples 2–5 was modified to investigate the main factors in the relaxivity of melanin. To confirm the basic effect of the binding of paramagnetic metals to melanin, melanin sample 3 was prepared with FeCl$_3$ (46 mmol/L) present in the initial reaction mixture (13-mmol/L L-dopa). Melanin typically aggregates and precipitates in the presence of metal and at low pH (7); this was expected to affect the relaxivities of melanin. To determine whether the known weak diamagnetism of metalfree melanin and the strong paramagnetism of metallomelanin depend on solubility, which theoretically determines the accessibility of their subunits (ligands) to solvent water molecules, melanin samples 2 (metalfree) and 4 (metal containing) were solubilized with meglumine (38 mmol/L), while melanin samples 1 (metalfree) and 3 (metal containing) were not. To determine the dependency of the relaxivities on the type of metal ion, melanin sample 4 was prepared with FeCl$_3$ (15 mmol/L) in the initial reaction mixture and melanin sample 5 with CuCl$_2$ (8 mmol/L) in the initial reaction mixture (8-mmol/L L-dopa for both).

The syntheses of melanin samples 6–9 were modified to investigate the main factors that control the iron-binding capacity of ferromelanin. To determine whether the binding capacity of melanin depends on when exposure to the iron occurs, melanin sample 4 was prepared with FeCl$_3$ (15 mmol/L) present in the initial reaction mixture (8 mmol/L L-dopa), while melanin sample 7 was prepared by slowly adding FeCl$_3$ (92 mmol/L) for several minutes to metalfree melanin (25 mg/mL). For all other comparisons, FeCl$_3$ (92 mmol/L) similarly was added to metalfree melanin (25 mg/mL). To determine whether the binding capacity depends on the mechanism of melanin synthesis, melanin samples 6 and 7 were prepared by means of autooxidation and melanin samples 8 and 9 by means of enzymatic oxidation, after which, in both cases, FeCl$_3$ was slowly added over several minutes. To determine the pH dependency of the binding capacity, FeCl$_3$ was slowly added to melanin samples 6 and 8 at pH 2 but to melanin samples 7 and 9 at pH 8.

In addition to increasing the solubility of melanin in the presence of metals and at low pH, the meglumine in all but one melanin preparation (melanin sample 3) was expected to complex with ionic iron, which would prevent its precipitation as an insoluble hydroxide at pH 8 while allowing transchelation to melanin (the much stronger chelator) and dialysis of any iron unbound to melanin. Melanin samples 1–5 were purified by means of exhaustive dialysis against deionized, distilled water, while melanin samples 6 and 8 were dialyzed in meglumine (38 mmol/L) at pH 2 and melanin samples 7 and 9 in meglumine (38 mmol/L) at pH 8. The molecular weight cutoff of 12,000–14,000 for the dialysis tubing permitted dialysis of low-molecular-weight fragments of melanin.

Chemical Analysis

Samples of each lyophilized melanin were weighed (Mettler Instrument, Highstown, NJ) and sent to an independent, outside laboratory to determine the iron or copper content (Galbraith Laboratories, Knoxville, Tenn). The metal contents of the samples were expressed as milligrams of
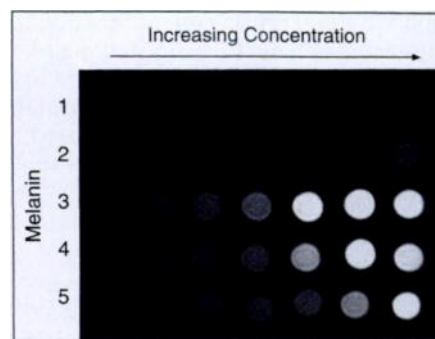

Figure 1. T1-weighted SE MR image (300/11) of melanin phantoms. The concentration of melanin increases from left to right (from 0.04 mg/mL to 20 mg/mL). Melanin samples 1 and 2, which are metalfree preparations, show little change in MR signal intensity with increasing concentration, except at the highest concentrations of melanin sample 2. In contrast, melanin samples 3–5, which are extensively dialyzed metallomelanins (no free metals in solution), show a substantial increase in signal intensity with increasing concentration. Melanin sample 3 has the highest signal intensities overall.

metal per milligram of solid sample. The basic procedure consists of charring the sample with H$_2$SO$_4$, solubilizing the metals present by refluxing in HNO$_3$, and measuring the metal concentration with inductively coupled plasma emission spectroscopy. The reported precision and accuracy of the technique are 3.1% and −1.6%, respectively (written communication, Galbraith Laboratories, 1997).

Relaxation Measurements

Longitudinal and transverse relaxation rates were determined for all samples by using a Nuclear Magnetic Spectrospin 120 Minispec nuclear MR analyzer (Bruker, Rheinstetten, Germany) that operates at 0.47 T (20 MHz) and 37°C. Lyophilized melanin was redissolved and serially diluted in deionized, distilled water to concentrations of 0.5–18.6 mg of solid per milliliter. The samples were maintained in a water bath at 40°C until the measurements
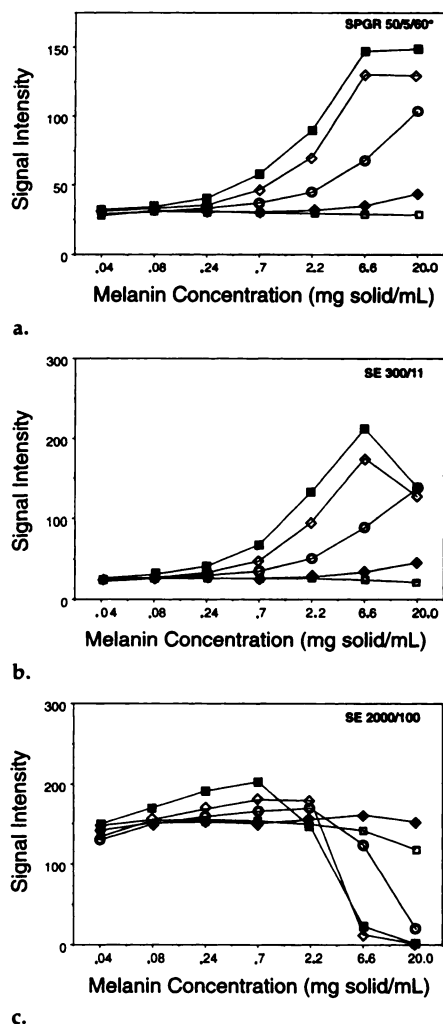
a.

SPGR 50/5/60°

Signal Intensity — 0, 50, 100, 150

Melanin Concentration (mg solid/mL) — .04 .08 .24 .7 2.2 6.6 20.0

b.

SE 300/11

Signal Intensity — 0, 100, 200, 300

Melanin Concentration (mg solid/mL) — .04 .08 .24 .7 2.2 6.6 20.0

c.

SE 2000/100

Signal Intensity — 0, 100, 200, 300

Melanin Concentration (mg solid/mL) — .04 .08 .24 .7 2.2 6.6 20.0

Figure 2. Dependence of the MR signal intensity of the metallomelanin phantoms on concentration for (a) T1-weighted spoiled gradient-recalled-echo (50/5; flip angle, 60°), (b) T1-weighted SE (300/11), and (c) T2-weighted SE (2,000/100) pulse sequences. Signal intensity is in arbitrary units. Melanin sample 1 = □, melanin sample 2 = ◆, melanin sample 3 = ■, melanin sample 4 = ◇, melanin sample 5 = ○.

were performed; their volumes were approximately 1.0 mL. Before each measurement, the spectrometer was tuned and calibrated.

T1 was measured by using an inversion-recovery pulse sequence, which yielded 20 data points that were fit to a monoexponential decay curve. This sequence was defined with an initial 180°—90° pulse separation of 5.0 msec and subsequent separations that increased by 30%.

T2 was measured from 75 data points generated by a Carr-Purcell-Meiboom-Gill pulse sequence with a 90°—180° pulse separation of 250 μsec. An echo time of 0.5 msec was used to minimize the residual T2* losses due to water diffusion through field gradients that may occur at longer echo times; this was important because of potential T2* effects from the aggregation of melanin that could occur despite the addition of meglumine in the presence of

metal ions at low pH (melanin samples 6 and 8). T2 was determined by fitting these data points to a monoexponential decay curve.·

Finally, 1/T1 and 1/T2 were plotted as functions of the concentration of metal (in micromoles of metal per milliliter) to determine the R1 and R2 values (in millimole of metal per liter per second) of the different experimental samples (melanin samples 3–9, FeCl₃, and iron diethylenetriaminepentaacetic acid [DTPA]).

Phantoms

To determine the relaxation behavior of the different melanin samples, phantoms were constructed for MR imaging. Lyophilized melanin was redissolved and diluted in meglumine (38 mmol/L) to varying concentrations (0.04, 0.08, 0.24, 0.7, 2.2, 6.6, or 20 mg of solid per milliliter of solution). The samples were then sealed and placed in a plastic sample holder until MR imaging was performed. Differences in signal intensity among the various samples were assessed by performing nonparametric Wilcoxon tests.

In preliminary experiments, two melanoma cell lines were grown in our laboratory: a melanotic line and an amelanotic line. The melanotic cell line (PC1A) was obtained from Ruth Halaban, PhD (Yale University, New Haven, Conn), and was used in several types of experiments. Cells were grown in Ham F-10 medium supplemented with 10% fetal bovine serum and with media changes every 3 days. Murine melanoma cells (B16) were isolated from fragments of tumor tissue obtained from the National Cancer Institute (Frederick, Md). The fragments were initially implanted into C57BL/6J mice (Charles River Breeding Laboratories, Wilmington, Mass).

To establish a viable line of cultured cells, tumors were dissected 10–14 days after implantation and aseptically homogenized in Dulbecco modified Eagle medium with 10% fetal bovine serum. Confirmation of cell viability by using trypan-blue exclusion showed that the suspension contained approximately 5×10^5 cells, which were resuspended in 15 mL of Dulbecco modified Eagle medium with 20% fetal bovine serum and placed into 250T tissue culture flasks that had been covered with 1% gelatin. By the 4th day, 85% of cells were attached to the bottom of the flask. Nonadherent cells were removed, and from that day the medium was changed every 3 days. Cells were grown in several batches.

For the MR imaging experiment, before imaging, melanotic PC1A melanoma cells and amelanotic B16 melanoma cells were grown for 3 days in Ham F-10 medium that contained 0.83 mg Fe/L (1.5 μmol/L) and in media that contained additional iron at concentrations of 3.0 mg Fe/L (5.3 μmol/L) and 8.0 mg Fe/L (14 μmol/L). A 24-well tissue culture plate was covered with 1% agarose in water (1.5 mL per well). On the day of phantom preparation, the cells were gently scraped with a cell

rake (Costar, Cambridge, Mass), washed with Hanks balanced salt solution, and counted with a hemocytometer (Fisher Scientific, Pittsburgh, Pa). Next, 3×10^6 cells from each tissue culture flask were resuspended in 30 μL of 1% agarose, and each such aliquot was placed into a small stenciled hole made in the agarose in the individual wells of the tissue culture plate. Each well was then covered with an additional layer of agarose to seal the cell pellets against drying and to preclude susceptibility artifacts due to air.

MR Imaging

MR imaging experiments were performed with a superconducting magnet system at 1.5 T (Signa 5.0; GE Medical Systems, Milwaukee, Wis). Melanin and melanoma phantoms were imaged in the coronal plane by using two T1-weighted pulse sequences and one T2-weighted sequence. The most T1-weighted sequence consisted of a spoiled gradient-recalled-echo sequence with 50/5 (a repetition time of 50 msec and an echo time of 5 msec), a 60° flip angle, and two signals acquired; the other T1-weighted sequence was a spin-echo (SE) sequence with 300/11 and four signals acquired.

The T2-weighted sequence was an SE sequence with 2,000/100 and two signals acquired. All images were acquired with a 5-inch surface coil, a 128×256 matrix, a 12-cm field of view, and a section thickness of 3 mm—except for the spoiled gradient-recalled-echo sequence, in which the section thickness was 0.7 mm. The signal intensities of the cell pellets were determined electronically and scaled to the signal intensity of the adjacent agarose within each well to calculate the signal-to-noise ratio.

RESULTS

Metal-binding Capacities of Synthetic Metallomelanins

The Table shows that the metal-binding capacities of the different synthetic metallomelanins vary considerably. The iron-binding capacities ranged from 0.03 mg of iron per milligram of solid (3% wt/wt) for melanin sample 7 to 0.16 mg of iron per milligram of solid (16% wt/wt) for melanin sample 4. The copper-binding capacity was approximately twofold higher than the highest iron-binding capacity (35% wt/wt for melanin sample 5 versus 16% wt/wt for melanin sample 4).

Overall, the iron-binding capacities were highest for the ferromelanins prepared by means of autooxidation in the presence of iron (melanin samples 3 and 4) and for those prepared by means of enzymatic oxidation and to which iron was subsequently added (melanin samples 8 and 9). By contrast, the binding capacities were lowest for those prepared by means of autooxidation but

to which the iron was added after synthesis (melanin samples 6 and 7). More specifically, the binding capacity was greater when the melanin was solubilized with meglumine (melanin samples 4 versus 3), when the iron was present during autooxidation (melanin samples 3 and 4) rather than when iron was added to metalfree melanin (melanin samples 6 and 7), when the melanin was produced by means of enzymatic oxidation (melanin samples 8 and 9) rather than by means of autooxidation (melanin samples 6 and 7), and when the iron was added at pH 2 (melanin samples 6 and 8) rather than pH 8 (melanin samples 7 and 9).

Relaxivities of Synthetic Metallomelanins

The Table shows that R1 and R2 for the different synthetic metallomelanins also varied considerably. The R1 for the ferromelanins ranged from $0.08 \ mmol \cdot L^{-1} \cdot sec^{-1}$ for melanin sample 8 to $1.02 \ mmol \cdot L^{-1} \cdot sec^{-1}$ for melanin sample 3; the R2 for the ferromelanins ranged from $0.24 \ mmol \cdot L^{-1} \cdot sec^{-1}$ for melanin sample 9 to $1.52 \ mmol \cdot L^{-1} \cdot sec^{-1}$ for melanin sample 7. When compared to the R1 of free iron ($7.2 \ mmol \cdot L^{-1} \cdot sec^{-1}$), that of the ferromelanin with the highest relaxivity (melanin sample 3, $1.02 \ mmol \cdot L^{-1} \cdot sec^{-1}$) is considerably lower but comparable to that of chelated Fe-DTPA ($0.97 \ mmol \cdot L^{-1} \cdot sec^{-1}$). It is interesting that, of the ferromelanins prepared by means of autooxidation, that with the highest iron-binding capacity (melanin sample 4) had the lowest relaxivities (an R1 of $0.34 \ mmol \cdot L^{-1} \cdot sec^{-1}$ and an R2 of $0.43 \ mmol \cdot L^{-1} \cdot sec^{-1}$). Despite having a much higher metal-binding capacity than the highest of the ferromelanins (35% wt/wt versus 16% wt/wt), cupromelanin had much lower relaxivities than the lowest of the ferromelanins (an R1 of $0.03 \ mmol \cdot L^{-1} \cdot sec^{-1}$ and an R2 = $0.06 \ mmol \cdot L^{-1} \cdot sec^{-1}$ vs an R1 of $0.08 \ mmol \cdot L^{-1} \cdot sec^{-1}$ and an R2 of $0.27 \ mmol \cdot L^{-1} \cdot sec^{-1}$).

Overall, the relaxivities were highest for the ferromelanin prepared by means of autooxidation with the iron present in the initial reaction mixture but without added meglumine (melanin sample 3) and for the ferromelanin in which the iron was added to metalfree melanin in the presence of meglumine (melanin sample 7). By contrast, the relaxivities were lowest for the ferromelanins prepared by means of enzymatic oxidation regardless of the

pH at which the iron was added (melanin samples 8 and 9). More specifically, the relaxivities were higher when the melanin was not solubilized by meglumine (melanin sample 3 vs 4), when the iron was added to metalfree melanin (melanin sample 7) rather than present during autooxidation (melanin sample 4), when the melanin was produced by means of autooxidation (melanin samples 6 and 7) rather than by means of enzymatic oxidation (melanin samples 8 and 9), and when the iron was added at pH 8 (melanin samples 7 and 9) rather than at pH 2 (melanin samples 6 and 8).

MR Imaging of Synthetic Melanin Phantoms

Figure 1 shows a T1-weighted SE MR image (300/11) of selected melanin phantoms (melanin samples 1–5). The synthetic metalfree melanins (melanin samples 1 and 2) showed little change in MR signal intensity with increasing melanin concentration over a wide range (0.04–20 mg/mL), except at the highest concentrations of melanin sample 2. As expected from the relaxivity measurements, all of the metallomelanins showed higher signal intensities than the metalfree melanins, and the signal intensities increased with increasing concentration. Thus, melanin sample 3 had the highest signal intensities, and a detection limit of 0.24 mg of ferromelanin per milliliter was estimated by means of visual inspection of the image.

Figure 2 summarizes the signal intensities for the different metallomelanins imaged with three different pulse sequences. The synthetic metalfree melanins (melanin samples 1 and 2) showed little change in signal intensity with increasing concentration with any pulse sequence, except at the highest concentrations of melanin sample 2. By comparison, the metallomelanins (melanin samples 3–5) showed increases in signal intensity with increasing concentration with the T1-weighted sequence, with saturation of the signal intensity for melanin samples 3 and 4 at the highest concentration (20 mg of solid per milliliter) owing to a T2 effect. This T2 effect was confirmed in melanin samples 3–5 at concentrations above 2 mg/mL by using the T2-weighted sequence.

MR Imaging of Melanoma Cell Phantoms

Both the melanotic PC1A and the amelanotic B16 melanoma cells were shown to be stable over several gen-
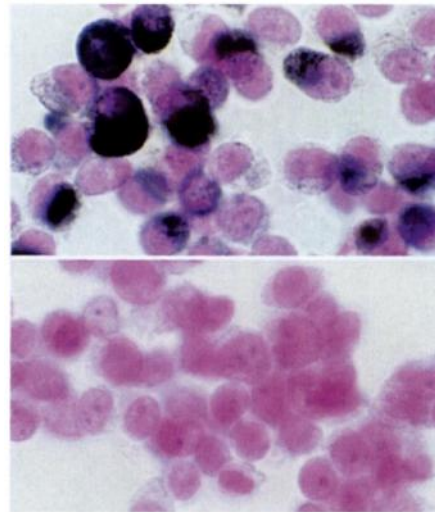

Figure 3. Melanotic PC1A (top) and amelanotic B16 (bottom) cultured melanoma cells. Melanin appears as tiny black granules scattered throughout the cytosol. (Fontana stain; original magnification, ×100.)

erations. Figure 3 shows the cytologic appearance of the two cell lines after staining with the Fontana stain for melanin, which is based on the ability of melanin to reduce silver nitrate to metallic silver. The PC1A cells thus contain innumerable darkly staining melanin granules (melanosomes), whereas the B16 cells do not. The melanotic melanoma cells grown in conventional medium or medium that contained additional iron had a substantially higher signal intensity than the amelanotic melanoma cells (Fig 4). It is important that the signal intensity of the melanotic melanoma cells increased with increasing concentration of iron in the media (for 0.83 mg Fe/L, the signal intensity [mean |in arbitrary units| ± standard deviation] was 786 ± 45; for 3.0 mg Fe/L, 952 ± 61; for 8.0 mg Fe/L, 1,064 ± 34), whereas it remained constant for the amelanotic melanoma cells (for 0.83 mg Fe/L, the signal intensity was 658 ± 25; for 3.0 mg Fe/L, 678 ± 23; for 8.0 mg Fe/L, 686 ± 26).

DISCUSSION

The results of this study show that the high MR signal intensity of synthetic metallomelanin on T1-weighted MR images is due primarily to bound paramagnetic metal. The small but definite increase in signal intensity for the highest concentrations of the metalfree melanin solubilized with meglumine (melanin sample 2) is consistent with a known weak diamagnetic effect (7). The former observation also is true for melanoma cells grown in
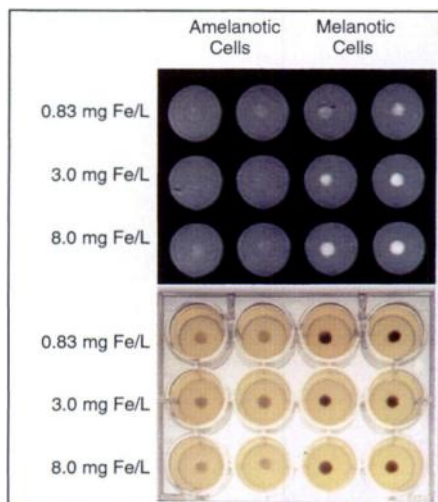
Figure 4. T1-weighted SE MR image (top; 300/11) and photograph (bottom) of melanoma cell phantoms (3×10^6 cells per well). All experiments were performed in duplicate. The first two columns represent amelanotic melanoma cells and the last two columns represent melanotic melanoma cells. The iron concentration in the incubation medium was 0.83 mg Fe/L (top row on the MR image and on the photograph), 3.0 mg Fe/L (middle row), or 8.0 mg Fe/L (bottom row). Cell pellets of the melanotic cell line (two right columns) show increases in MR signal intensity with increasing iron concentration, whereas those of the amelanotic cell line (two left columns) do not. The melanotic cells appear dark brown owing to their pigment content. Differences in signal intensities between the pellets of melanotic cells in columns 3 and 4 are due to variations in cell clumping within each pellet and in the volume of each pellet included in this single 3-mm-thick imaging section.

Figure 5. Melanin chelating groups. Metal-chelate complexes formed with a generic subunit in melanin as a function of pH. Me = metal.

conventional medium or medium that contains additional iron, in which the signal intensity increases when melanin is present in the cells but not when it is absent. These results are direct evidence that natural melanin in cells scavenges metals and show that the binding of paramagnetic metals by natural melanin can be monitored with MR imaging.

Melanins and Melanogenesis

Melanins are a group of biopolymeric pigments found in animals and plants, where their best understood roles are in coloration and photoprotection (21). A more recent hypothesis is that melanin has an additional cytoprotective function as a scavenger of toxic substances such as metals (15). Animal melanins are classified into two major groups according to their predominant precursors: brown-black eumelanin and red-yellow pheomelanin (21–23). Melanins are unusual among the biopolymers in that they are highly polyanionic, cross-linked,
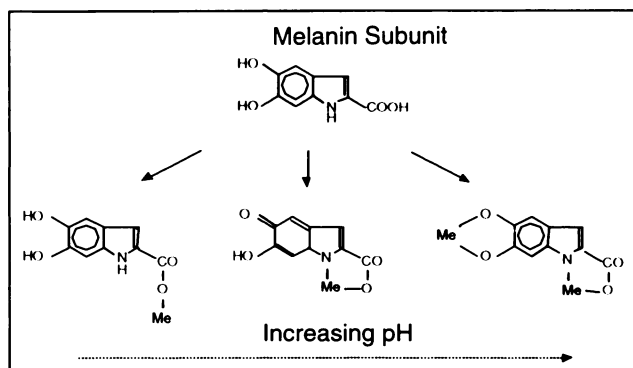
and heterogeneous polymers (22–24). Melanins also are unique in that they contain a stable population of organic free radicals (25). Natural melanins are synthesized within the melanosome, a specialized organelle of the melanocytes in pigmented tissues, according to established biochemical pathways and regulatory controls (21,26,27).

The melanosomal enzyme tyrosinase (monophenol or 3,4-dihydroxyphenylalanine oxygen oxidoreductase [EC 1.14.18.1]) has a central role in melanogenesis because it catalyzes the initial two reactions: the hydroxylation of tyrosine to form dopa (not rate limiting) and the subsequent oxidation of dopa to form dopaquinone (rate limiting) (28). The latter undergoes spontaneous cyclization to form leucodopachrome, which then oxidizes to form dopachrome. Subsequently, dopachrome is reduced to the form 5,6-dihydroxyindole-2-carboxylic acid, which then decarboxylates through the enzymatic action of dopachrome tautomerase, through catalysis by zinc, or through both to form 5,6-dihydroxyindole. The classic Raper-Mason scheme for eumelanogenesis predicts that 5,6-dihydroxyindole and 5,6-dihydroxyindole-2-carboxylic acid ultimately oxidize and polymerize to form a homogeneous copolymer (29,30). However, it is now known that all of the intermediates above, as well as those from competing side reactions and tyrosinase itself, can become incorporated before they react further, thus forming a highly heterogeneous polymer (22–24).

Metal Binding by Melanins

The wide (10-fold) variation in metal-binding capacities among the various synthetic metallomelanins in this study reflects the heterogeneous

structure of melanin and indicates that metal binding by melanin is a complex function of the synthetic conditions that determine the final structure of the melanin (and the types and numbers of binding sites), the metal and the stabilities of its complexes with the subunits of melanin, and whether the metal is present during or added after synthesis of the melanin. For example, the much higher binding capacity for copper than for iron probably reflects a more favorable ligand geometry for copper, which has the square-planar symmetry readily provided by ligands in melanin (9).

Several populations of metal-binding sites with differential binding affinities have been shown to exist in melanin, the strongest of which has a binding constant of 5.2×10^7 L/mol for manganese and occurs at 0.07 mmol/mg melanin (8,9,31). Other binding sites are more abundant (up to 1.2 μmol per milligram of melanin) but have lower affinities (ranging from 1.8×10^6 to 1.1×10^3 L/mol for manganese) (8,9,31). Quantitative binding affinities of melanins have not been determined for other metal ions. The major ligands through which metals bind to melanin are carboxylate, aromatic hydroxyl, and amine groups. The metal chelate complexes formed by a generic subunit in melanin are summarized in Figure 5, which shows their typical square-planar symmetry and indicates that their proportions depend on pH (9). At physiologic pH, the predominant complex involves chelation by the indole nitrogen and carboxylate side chain.

Relaxivities of Metallomelanins

In general, the relaxation rates of solutions have two major contributors: relatively strong "inner sphere" relaxation, which arises when solvent

water molecules bind to a solute for a time long enough to form an identifiable chemical complex, and relatively weak "outer sphere" relaxation, which arises when the water molecules diffuse nearby but do not become bound to this complex (32). For paramagnetic complexes in solution at typical imaging fields, inner-sphere relaxation predominates and depends both on the number of sites on the metal available for coordination with water molecules and the rotational correlation time of the complex. Although the formation of a chelate complex between a paramagnetic aquo ion and a macromolecular chelator reduces the number of coordination sites on the metal available for inner-sphere exchange with water molecules, the reduction in rotational correlation time of the metal due to binding causes an overall marked increase in relaxation rates. Nuclear magnetic relaxation dispersion profiles (plots of the relaxation rate versus the magnetic field strength or Larmor frequency) of paramagnetic metals bound to synthetic melanins are homologous to those obtained for each metal when its aquo ion becomes immobilized by binding to any slowly rotating macromolecule (7).

The generally much higher relaxivities of the ferromelanins compared to the relaxivity of the single cupromelanin prepared in this study confirm prior published data that show that paramagnetic metals, when bound to melanin, have unequal effects on relaxation rates (7). For iron-protein complexes in general, the relaxivities vary substantially with the ligand configuration of the iron atoms but typically are low (33–36). In contrast, the relaxivity of melanin-bound iron is substantially higher than the relaxivities of most iron-containing proteins and is comparable to the unique case of fluoromethemoglobin (35). The high relaxivity of melanin-bound iron, by analogy, may be associated with the rapid exchange of water molecules hydrogen bonded to hydroxide ligands on the iron atoms, because the exchange of water molecules coordinated to iron typically is slow.

The wide (10-fold) variation in relaxivities among the various synthetic ferromelanins in this study, like that of their iron-binding capacities, also reflects the structural heterogeneity of melanin and the complexity of its binding of metals. This variation indicates that the accessibility of bound metals in metallomelanins to solvent water molecules is dependent on the higher-order structure of the metallomelanin, which is a function of the

synthetic conditions and of the solubility of the metallomelanin. This is best illustrated by the observation that the ferromelanin prepared by means of autooxidation that had the highest iron-binding capacity (melanin sample 4, 16% wt/wt) had the lowest relaxivities (an R1 of 0.34 mmol · L⁻¹ · sec⁻¹ and an R2 of 0.43 mmol · L⁻¹ · sec⁻¹), possibly because a large fraction of the iron atoms was bound deep within the polymer and relatively inaccessible to solvent water molecules.

Importance and Future Studies

We provide further experimental evidence for the common radiologic observation that many melanomas have high signal intensity on T1-weighted MR images, and we confirm previous conclusions that the effect of natural melanin on T1 in vivo almost certainly is due to bound paramagnetic metals (7,16,17). In one of the later studies (7), quantitative data in the literature on the presence of metals bound to natural melanin in situ (12–14) have been combined with quantitative relaxivity data from model solutions of synthetic melanin to which the same metals had been added to show that melanin-bound iron has the dominant effect in vivo.

The results of this study show that ferromelanin indeed is readily detectable with MR imaging under realistic in vivo conditions. In particular, the estimated detection limit of 0.24 mg/mL for one of the synthetic ferromelanins (melanin sample 3) compares favorably with a published estimate of the average tissue concentration of melanin in melanoma of 15 mg/mL (7). Thus, it may be possible to exploit this scavenging property of natural melanin to increase the conspicuity of melanomas on nuclear images by administering radioactive metals such as gallium-67 or indium-111, which would accumulate in the melanin.

We are currently exploring a strategy for noninvasively monitoring gene therapy on the basis of the observations above and the fact that melanin synthesis is controlled in vivo by a single enzyme, tyrosinase, whose induction potentially can be controlled by means of genetic manipulation (see the companion article by Weissleder and colleagues [37]). This strategy consists of inserting the gene for mammalian tyrosinase into a plasmid vector that contains a therapeutic gene. Coexpression of the tyrosinase gene in the same reading frame as the therapeutic gene would lead to in situ synthesis of melanin, which would then passively

accumulate paramagnetic metals (either ubiquitous natural iron—present in the extracellular fluid at a concentration of 1 mg/mL—or an exogenous metal such as manganese, administered intravenously) and therefore be detectable with MR imaging. Thus, expression of the therapeutic gene theoretically could be detected and monitored via the concomitant production of melanin. Ongoing work toward refining this strategy is aimed at optimizing the synthesis of and purifying different natural melanins in cell culture, quantitating their metal-binding affinities and capacities, and quantitating metal accumulation by intracellular melanin in cultured cells exposed to exogenous metal chelates and investigating any associated cytotoxicity. ∎

References

1. Atlas S, Braffman B, LoBrutto R, Elder D, Herlyn D. Human malignant melanomas with varying degrees of melanin content in nude mice: MR imaging, histopathology, and electron paramagnetic resonance. J Comput Assist Tomogr 1990; 14:547–554.
2. Bilaniuk L, Atlas S, Zimmerman R. Magnetic resonance imaging of the orbit. Radiol Clin North Am 1987; 25:509–528.
3. Gomori J, Grossman R, Shields J, Augsburger J, Joseph P, DeSimeone D. Choroidal melanomas: correlation of NMR spectroscopy and MR imaging. Radiology 1986; 158:443–445.
4. Peyman G, Mafee M. Uveal melanoma and similar lesions: the role of magnetic resonance imaging and computed tomography. Radiol Clin North Am 1987; 25:471–486.
5. Atlas S, Grossman R, Gomori J, et al. MR imaging of intracranial metastatic melanoma. J Comput Assist Tomogr 1987; 11:577–582.
6. Aime S, Botta M, Ermondi G, Fasano M, Terreno E. Paramagnetic water proton relaxation enhancement: from contrast agents in MRI to reagents for quantitative "in vitro" assays. Magn Reson Imaging 1992; 10:849–854.
7. Enochs W, Hyslop W, Bennett H, Brown R, Koenig S, Swartz H. Proton relaxation rates in synthetic melanin solutions: implications for mechanisms of enhanced relaxation in melanotic melanoma. Invest Radiol 1989; 24:794–804.
8. Sarna T, Hyde J, Swartz H. Ion-exchange in melanin: an electron spin resonance study with lanthanide probes. Science 1976; 192:1132–1134.
9. Froncisz W, Sarna T, Hyde J. Cu2+ probe of metal-ion binding sites in melanin using electron paramagnetic resonance spectroscopy. I. Synthetic melanins. Arch Biochem Biophys 1980; 202:289–303.
10. Potts A, Au P. The affinity of melanin for inorganic ions. Exp Eye Res 1976; 22:487–491.
11. Sarna T, Froncisz W, Hyde J. Cu2+ probe of metal binding sites of melanin using electron paramagnetic resonance spectroscopy. II. Natural melanins. Arch Biochem Biophys 1980; 202:304–313.
12. Horcicko J, Borovansky J, Duchon J, Prochazkova B. Distribution of zinc and copper in pigmented tissues. Z Physiol Chem 1973; 354:203–204.

13. Parkinson T, Millikan L, Anderson D. Manganese, copper and zinc concentrations in human skin lesions. Int J Appl Radioisotopes 1979; 30:411–415.
14. Okazaki M, Kuwata K, Miki Y, Shiga S, Shiga T. Electron spin relaxation of synthetic melanin and melanin-containing human tissue as studied by electron spin echo and electron spin resonance. Arch Biochem Biophys 1985; 242:197–205.
15. Larsson B. Interaction between chemicals and melanin. Pigment Cell Res 1993; 6:127–133.
16. Tosk J, Holshouser B, Aloia R, et al. Effects of the interaction between ferric iron and L-dopa melanin on T1 and T2 relaxation times determined by magnetic resonance imaging. Magn Reson Med 1992; 26:40–45.
17. Aime S, Fasano M, Terreno E, Sarzanini C, Mentasti E. An NMR study of the interaction between melanin free acid and Mn2+ ions as a model to mimic the enhanced proton relaxation rates in melanotic melanoma. Magn Reson Imag 1991; 9:963–968.
18. Enochs W, Nilges M, Swartz H. Purified human neuromelanin, synthetic dopamine melanin as a potential model pigment, and the normal human substantia nigra: characterization by electron paramagnetic resonance (EPR) spectroscopy. J Neurochem 1993; 61:68–79.
19. Enochs W, Nilges M, Swartz H. A standardized test for the identification and characterization of melanins using electron paramagnetic resonance (EPR) spectroscopy. Pigment Cell Res 1993; 6:91–99.
20. Enochs W, Nilges M, Swartz H. The minocycline-induced thyroid pigment and several synthetic models: identification and characterization by electron paramagnetic resonance (EPR) spectroscopy. J Pharmacol Exp Ther 1993; 266:1164–1176.
21. Jimbow K, Quevedo W, Fitzpatrick T, Szabo G. Some aspects of melanin biology. J Invest Dermatol 1976; 67:72–89.
22. Swan G. Structure, chemistry and biosynthesis of the melanins. Fortsch Chem Org Naturst 1974; 31:521–582.
23. Prota G. Progress in the chemistry of melanins and related metabolites. Med Res Rev 1988; 8:525–556.
24. Blois M. The melanins: their synthesis and structure. In: Smith KC, ed. Photochemical and photobiological reviews. New York, NY: Plenum, 1978; 115–134.
25. Sealy R, Felix C, Hyde J, Swartz H. Structure and reactivity of melanins: influence of free radicals and metal ions. In: Prior WA, ed. Free radicals in biology. New York, NY: Academic Press, 1980; 209–259.
26. Jimbow K. Current update and trends in melanin pigmentation and melanin biology. Keio J Med 1995; 44:9–18.
27. Mishima Y. A post melanosomal era: control of melanogenesis and melanoma growth. Pigment Cell Res 1992; 2(suppl):3–16.
28. Sanches-Ferrer A, Rodriguez-Lopez J, Garcia-Canovas F, Garcia-Carnoma F. Tyrosinase: a comprehensive review of its mechanism. Biochim Biophys Acta 1995; 1247:1–11.
29. Raper H. Some problems of tyrosine metabolism. J Chem Soc London 1938; 125.
30. Mason H. Structure of melanins. In: Gordon M, ed. Pigment cell biology. New York, NY: Academic Press, 1959; 563–582.
31. Lyden A, Larsson B, Lindquist N. Melanin affinity of manganese. Acta Pharmacol Toxicol 1984; 55:133–138.
32. Koenig S. From the relaxivity of Gd-(DTPA)$^{2-}$ to everything else. Magn Reson Med 1991; 22:183–190.
33. Koenig S, Baglin C, Brown R. Magnetic field dependence of solvent proton relaxation in aqueous solutions of Fe3+ complexes. Magn Reson Med 1985; 2:283–288.
34. Koenig S, Schillinger W. Nuclear magnetic resonance relaxation dispersion in protein solutions. II. Transferrin. J Biol Chem 1969; 244:6520–6526.
35. Koenig S, Brown R, Lindstrom T. Interactions of solvent with the heme region of methemoglobin and fluoromethemoglobin. In: Chien H, ed. Hemoglobin and oxygen binding. New York, NY: Elsevier Biomed 1982; 377–385.
36. Koenig S, Brown R, Gibson J, Ward R, Peters T. Relaxometry of ferritin solutions and the influence of the Fe3+ core ions. Magn Reson Med 1986; 3:755–767.
37. Weissleder R, Simonova M, Bogdanova A, Bredow S, Enochs WS, Bogdanov A. MR imaging and scintigraphy of gene expression through melanin induction. Radiology 1997; 204:425–429.